

## Fluorinated Alcohols Enable Olefin Epoxidation by H<sub>2</sub>O<sub>2</sub>: Template Catalysis

Samuël P. de Visser,<sup>†</sup> Jose Kaneti,<sup>†</sup> Ronny Neumann,<sup>\*,‡</sup> and Sason Shaik<sup>\*,†</sup>

Department of Organic Chemistry and The Lise Meitner–Minerva Center for Computational Quantum Chemistry, Hebrew University, Givat Ram Campus, 91904 Jerusalem, Israel, and Department of Organic Chemistry, Weizmann Institute of Science, 76100 Rehovot, Israel

sason@yfaat.ch.huji.ac.il

Received January 24, 2003

Experimental observations show that direct olefin epoxidation by H<sub>2</sub>O<sub>2</sub>, which is extremely sluggish otherwise, occurs in fluorinated alcohol (R<sub>f</sub>OH) solutions under mild conditions requiring no additional catalysts. Theoretical calculations of ethene and propene epoxidation by H<sub>2</sub>O<sub>2</sub> in the gas phase and in the presence of methanol and of two fluorinated alcohols, presented in this paper, show that the fluoro alcohol itself acts as a catalyst for the reaction by providing a template that stabilizes specifically the transition state (TS) of the reaction. Thus, much like an enzyme, the fluoro alcohol provides a complementary charge template that leads to the reduction of the barrier by 5–8 kcal mol<sup>-1</sup>. Additionally, the fluoro alcohol template keeps the departing OH and hydroxyalkenyl moieties in close proximity and, by polarizing them, facilitates the hydrogen migration from the latter to form water and the epoxide product. The reduced activation energy and structural confinement of the TS over the fluoro alcohol template render the epoxidation reaction observable under mild synthetic conditions.

### Introduction

Hydrogen peroxide is an environmentally friendly oxidant and is therefore touted as a synthetic reagent. Like all peroxides, H<sub>2</sub>O<sub>2</sub> possesses a low O–O bond energy<sup>1,2</sup> and therefore, in principle, is a good oxygen donor provided it can be activated by a catalyst. The catalyzed oxygenation mechanisms by H<sub>2</sub>O<sub>2</sub> and related peroxides pose some intriguing mechanistic puzzles. Some controversy still surrounds the issue of whether the mechanism of oxygen insertion into C=C and C–H bonds by, e.g., peroxyacids is homolytic or heterolytic. Strong acids protonate the peroxide and promote a heterolytic mechanism. Indeed, experimental and computational studies indicate that protonated hydrogen peroxide, H<sub>3</sub>O<sub>2</sub><sup>+</sup>, is a very powerful oxidant.<sup>3,4</sup> By contrast, weak acids such as CF<sub>3</sub>COOH appear to participate in the activation of H<sub>2</sub>O<sub>2</sub> in their nondissociated forms and catalyze the oxygen insertion by hydrogen bonding to the oxidant.<sup>5</sup> Recently, one of us<sup>6</sup> and others<sup>7</sup> have

demonstrated that 1-octene, which is notoriously difficult to epoxidize, undergoes epoxidation under mild conditions when H<sub>2</sub>O<sub>2</sub> is employed in fluorinated alcoholic solutions, e.g., CF<sub>3</sub>CH<sub>2</sub>OH and (CF<sub>3</sub>)<sub>2</sub>CHOH. No acid catalysis of the reaction was necessary, since the epoxidation takes place when commercial H<sub>2</sub>O<sub>2</sub> is buffered with 0.05 equiv of Na<sub>2</sub>HPO<sub>4</sub>, a quantity more than sufficient to neutralize the stabilizing sulfuric acid additive,<sup>7</sup> or used at pH = 8 by addition of sodium carbonate.<sup>6b</sup> In addition, in the presence of the fluoro alcohols, the reaction of hydrogen peroxide with *cis*-stilbene gave complete retention of the olefin configuration.<sup>6</sup> By contrast, no reaction of H<sub>2</sub>O<sub>2</sub> with olefins is observed in ethanol or 2-propanol.<sup>6</sup> The lack of reactivity in common solvents and, in particular, nonfluorinated alcohols<sup>6</sup> suggests that fluorine plays a key role in promoting the epoxidation.<sup>8</sup> *What is this role of fluorine, and what are the factors that enable alkene epoxidation by H<sub>2</sub>O<sub>2</sub> in the presence of fluoro alcohols?* We address these questions in the present study by theoretical means.

### Outline of Theoretical Strategy

Hydrogen bonding in peroxides has already been shown as an important factor contributing to the stereochemical course of olefin epoxidation.<sup>9–11</sup> An initial lead to the activation of hydrogen peroxide by fluoro alcohols

\* To whom correspondence should be addressed (S.S.): Tel. +972-2-6585909, Fax +972-2-658-4680.

<sup>†</sup> Hebrew University.

<sup>‡</sup> Weizmann Institute of Science.

(1) *Peroxide Reaction Mechanisms*, Edwards, J. O., Ed.; Interscience: New York, 1962; pp 67–106.

(2) Bach, R. D.; Ayala, P. Y.; Schlegel, H. B. *J. Am. Chem. Soc.* **1996**, *118*, 12758–12765.

(3) Øiestad, E. L.; Harvey, J. N.; Uggerud, E. *J. Phys. Chem. A* **2000**, *104*, 8382–8388.

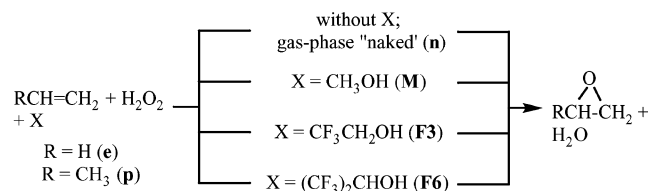
(4) Øiestad, Å. M. L.; Petersen, A. C.; Bakken, V.; Vedde, J.; Uggerud, E. *Angew. Chem., Int. Ed.* **2001**, *40*, 1305–1309.

(5) Bach, R. D.; Canepa, C.; Winter, J. E.; Blanchette, P. E. *J. Org. Chem.* **1997**, *62*, 5191–5197.

(6) (a) Neimann, K.; Neumann, R. *Org. Lett.* **2000**, *2*, 2861–2863. (b) Neimann, K.; Neumann, R. Unpublished data.

(7) van Vliet, M. C. A.; Arends, I. W. C. E.; Sheldon, R. A. *Synlett* **2001**, 248.

(8) (CF<sub>3</sub>)<sub>2</sub>CHOH was found also to potentiate benzenearsonic acid as a catalyst of hydrogen peroxide promoted epoxidation of 1-octene epoxidation. See: Berkessel, A.; Andrae, M. R. M. *Tetrahedron Lett.* **2001**, *42*, 2293–2295.

**SCHEME 1. Model Epoxidation Reactions Studied to Reveal the Effect of Fluoro Alcohols**


could have therefore been associated with the hydrogen bonding capability of these solvents with the oxidizing reagent. Thus, fluorinated alcohols are known to form multiple hydrogen-bonded complexes that affect sugar conformations and secondary structures of biopolymers.<sup>12,13</sup> Infrared spectroscopic experiments and theoretical calculations<sup>14–16</sup> showed that hydrogen peroxide is both a better proton donor and a better proton acceptor than water. Some more support is provided by the <sup>1</sup>H and <sup>17</sup>O NMR spectra of H<sub>2</sub>O<sub>2</sub> in fluorinated alcohols, which clearly indicate<sup>6</sup> the complexation between H<sub>2</sub>O<sub>2</sub> and the fluorinated alcohols. It was surmised<sup>6</sup> that in these complexes fluorine acts as a hydrogen bond acceptor and the slightly acidic alcoholic hydroxyl as hydrogen bond donor. Our preliminary tests, using GIAO-B3LYP/6-311++G\*\* calculations of complexes of fluorinated alcohols and H<sub>2</sub>O<sub>2</sub> confirm the NMR findings<sup>6a</sup> that the fluoro alcohol (R<sub>f</sub>OH) is capable of acting as both a proton donor and a proton acceptor (see Supporting Information). Thus, the lack of reactivity in nonfluorinated alcohols<sup>6a</sup> and the fact that fluoro alcohols are nonpolar solvents with lower dielectric constants compared with their nonfluorinated analogues suggest that the observed catalysis of epoxidation is not due to a general "solvent effect". *The fluorine substituents must be playing a key role in stabilizing the transition state*, and therefore the fluoro alcohol should be explicitly included in the calculations.

To address these issues, we studied ethene and propene epoxidation by H<sub>2</sub>O<sub>2</sub>, in either "naked" form or in the presence of methanol, trifluoroethanol, or hexafluoroisopropyl alcohol. Scheme 1 shows the model reactions and the adopted notations; **n** stands for "naked" H<sub>2</sub>O<sub>2</sub>, **F3** for CF<sub>3</sub>CH<sub>2</sub>OH-H<sub>2</sub>O<sub>2</sub>, **F6** for H<sub>2</sub>O<sub>2</sub>-(CF<sub>3</sub>)<sub>2</sub>CHOH, and **M** for methanol, and the labels **e** and **p** stand for ethene and propene, respectively. The reactions of the naked system and that in the presence of methanol will serve as reference reactions, which will enable estimation of the effect of the fluorinated alcohols. On the basis of

Scheme 1, the various species are labeled by letter combinations, where **C**, **TS**, and **P** stand for oxidant clusters, transition structures, and products. For example, **C(F3)** is the oxidant cluster of trifluoroethanol with H<sub>2</sub>O<sub>2</sub>, **TS(e,n)** refers to the transition structure of the naked system for ethene epoxidation, **TS(p,F6)** refers to the transition structure of propene epoxidation catalyzed by hexafluoro-2-propanol, etc.

**Methods and Computational Details**

**Method Selection.** Oxidation by peroxides is known to exhibit trends that are compatible with either concerted polar reactions or with stepwise biradical mechanisms through O–O bond homolysis.<sup>17</sup> This poses computational difficulties in distinguishing between the mechanisms,<sup>18</sup> which were discussed thoroughly<sup>19</sup> in a recent paper on the oxygen insertion reaction of dioxiranes to C–H bonds. Thus, it was shown<sup>19</sup> that using restricted DFT (RDFT) or unrestricted DFT (UDFT) calculations gives rise to different mechanisms; RDFT leads to a concerted oxygenation, whereas UDFT leads to a stepwise mechanism via diradical intermediates. All RDFT transition states (TSs) were found to exhibit instability with respect to alternative UDFT solutions. The latter lead to stepwise mechanisms and, in most systems, also to considerably lower lying TSs. As a result of technical procedures in GAUSSIAN-98,<sup>20</sup> performing a UDFT calculation on the converged RDFT structure gives the same RDFT solution back. However, a proper UDFT calculation can be initiated by subjecting the TS from an RDFT calculation to a stability check. Accordingly we performed RDFT calculations and subjected all of them to a stability check to subsequently explore the UDFT surfaces for two reactions.

**Computational Details.** RDFT calculations on model alkene epoxidations with the hybrid B3LYP functional were carried out using the standard Gaussian basis sets,

(17) For arguments and counter arguments for the oxygen transfer reactions of dioxiranes, see: (a) Adam, W.; Curci, R.; D'Accolti, L.; Dinoli, A.; Fusco, C.; Gasparrini, F.; Kluge, R.; Paredes, R.; Schulz, M.; Smerz, A. K.; Velloza, L. A.; Weinkotz, S.; Winde, R. *Chem. Eur. J.* **1997**, *3*, 105. (b) González-Núñez, M. E.; Castellano, G.; Andreu, C.; Royo, J.; Báguena, M.; Mello, R.; Asensio, G. *J. Am. Chem. Soc.* **2001**, *123*, 7487–7491. (c) Bravo, A.; Fontana, F.; Fronza, G.; Minisci, F.; Zhao, L. *J. Org. Chem.* **1998**, *63*, 254–263.

(18) For computational results that favor concerted vs stepwise oxygenation by dioxiranes, see: (a) Glukhovtsev, M. N.; Canepa, C.; Bach, R. D. *J. Am. Chem. Soc.* **1998**, *120*, 10528–10533. (b) Du, X.; Houk, K. N. *J. Org. Chem.* **1998**, *63*, 6480–6483. (c) Fokin, A. A.; Tkachenko, B. A.; Korshunov, O. I.; Gunchenko, P. A.; Schreiner, P. R. *J. Am. Chem. Soc.* **2001**, *123*, 11248–11252. (d) Shustov, G. V.; Rauk, A. *J. Org. Chem.* **1998**, *63*, 5413–5422.

(19) For a recent discussion of the issues concerning the use of UDFT and RDFT method for oxygen insertion by dioxiranes, see: Freccero, M.; Gandolfi, R.; Sarzi-Amadè, M.; Rastelli, A. *J. Org. Chem.* **2003**, *68*, 811–823.

(20) Frisch, M. J.; Trucks, G. W.; Schlegel, H. B.; Scuseria, G. E.; Robb, M. A.; Cheeseman, J. R.; Zakrzewski, V. G.; Montgomery, J. A., Jr.; Stratmann, R. E.; Burant, J. C.; Dapprich, S.; Millam, J. M.; Daniels, A. D.; Kudin, K. N.; Strain, M. C.; Farkas, O.; Tomasi, J.; Barone, V.; Cossi, M.; Cammi, R.; Mennucci, B.; Pomelli, C.; Adamo, C.; Clifford, S.; Ochterski, J.; Petersson, G. A.; Ayala, P. Y.; Cui, Q.; Morokuma, K.; Malick, D. K.; Rabuck, A. D.; Raghavachari, K.; Foresman, J. B.; Cioslowski, J.; Ortiz, J. V.; Stefanov, B. B.; Liu, G.; Liashenko, A.; Piskorz, P.; Komaromi, I.; Gomperts, R.; Martin, R. L.; Fox, D. J.; Keith, T.; Al-Laham, M. A.; Peng, C. Y.; Nanayakkara, A.; Gonzalez, C.; Challacombe, M.; Gill, P. M. W.; Johnson, B. G.; Chen, W.; Wong, M. W.; Andres, J. L.; Head-Gordon, M.; Replogle, E. S.; Pople, J. A. *Gaussian 98*, revision A.7; Gaussian, Inc.: Pittsburgh, PA, 1998.

(9) Freccero, M.; Gandolfi, R.; Sarzi-Amadè, M.; Rastelli, A. *J. Org. Chem.* **1999**, *64*, 3853–3860.

(10) Adam, W.; Bach, R. D.; Dmitrenko, O.; Saha-Möller, C. R. *J. Org. Chem.* **2000**, *65*, 6715–6728.

(11) Washington, I.; Houk, K. N. *Angew. Chem., Int. Ed.* **2001**, *40*, 4485–4488.

(12) Hong, D.-P.; Hoshino, M.; Kuboi, R.; Goto, Y. *J. Am. Chem. Soc.* **1999**, *121*, 8427–8433.

(13) (a) Buck, M. *Quart. Rev. Biophys.* **1998**, *31*, 297–355. (b) Fioroni, M.; Burger, K.; Mark, A. E.; Roccatano, D. *J. Phys. Chem. B* **2000**, *104*, 12347–12354.

(14) Rankin, K. N.; Boyd, R. J. *J. Comput. Chem.* **2001**, *22*, 1590–1597.

(15) (a) Mó, O.; Yáñez, M.; Rozas, I.; Elguero, J. *J. Chem. Phys.* **1994**, *100*, 2871–2877. (b) Mó, O.; Yáñez, M.; Rozas, I.; Elguero, J. *Chem. Phys. Lett.* **1994**, *219*, 45–52.

(16) (a) Goebel, J. R.; Ault, B. S.; Del Bene, J. E. *J. Phys. Chem. A* **2000**, *104*, 2033–2037. (b) Goebel, J. R.; Ault, B. S.; Del Bene, J. E. *J. Phys. Chem. A* **2001**, *105*, 11365–11370.

6-311++G\*\*. A few calculations were tried also with 6-311G\*\*, which was abandoned in favor of the more extended basis set. The reaction critical points for the epoxidation pathways in Scheme 1 were studied by gradient optimization. All the TSs were verified by frequency calculations. The reaction mechanisms for the smaller systems, (e,n) and (e,F3) were ascertained by intrinsic reaction coordinate (IRC) following.<sup>21,22</sup> Partial charges were determined using NBO analysis.<sup>23</sup>

Two types of critical structures were located during the TS search. The initial structure, leading to a synchronous-concerted epoxidation (two equal C–O bonds), was found to be a second-order saddle point, having two imaginary frequencies. One of the frequencies is a cartwheel rotation that leads to a structure with unequal C–O bonds. This latter structure was characterized as a first-order saddle point with a single imaginary frequency, namely, a genuine TS. Locating initially the second-order saddle point proved useful for an eventual location of the real TSs. The so obtained RDFT TSs that were found to correspond to concerted epoxidations were subsequently subjected to instability checks and gave lower UDFT solutions. These results are discussed later, but already at this point it is important to emphasize that the RDFT-UDFT energy differences are exceedingly small (0.03–2.26 kcal mol<sup>-1</sup>) for the transition states that include the fluoro alcohol molecules. Furthermore, inclusion of solvent polarity effect (see below) reverses the order in favor of the corresponding RDFT structures. Finally, as shown later, the RDFT and UDFT conclusions concerning the effect of the fluoro alcohol are after all very similar.

A few MP2 calculations were attempted and showed that the concerted TSs found with DFT could also be located with MP2. However, the MP2 method was abandoned because its frequency calculations with R<sub>f</sub>OH were extremely time-consuming and repeatedly crashed. The MP2 data is collected in Supporting Information. The following text is restricted to the description of the B3LYP/6-311++G\*\* results, and other data are presented in Supporting Information.

**Reference Reactions.** To assess the effect of fluorinated alcohols, we tested two reference model reactions. One is the reaction of the naked H<sub>2</sub>O<sub>2</sub>, labeled **n** in Scheme 1 above. The other, labeled **M**, involves a non-fluorinated alcohol, CH<sub>3</sub>OH. Therefore, the naked (**n**) gas-phase reaction and the one assisted by methanol (**M**) were adopted as models of the noncatalyzed epoxidation, while reactions **F3** and **F6** address the catalytic effect of fluorinated alcohols and the possible role of fluorine as a hydrogen bonding acceptor.<sup>6–8,12,13</sup> To have a more realistic estimate of the catalytic effect, we computed the effect of solvent polarity on the barriers through single point calculations. The solvent calculations were done with the implementation of the polarized continuum model in JAGUAR 4.1.<sup>24</sup> The solvent is characterized by two quantities, its dielectric constant ( $\epsilon$ ) and the probe radius ( $r$ ). We used two solvents with  $\epsilon = 5.708$ ,  $r = 2.72$

Å and  $\epsilon = 10.65$  and  $r = 2.51$  Å. These dielectric constants bracket the value ( $\epsilon = 8.55$ ) for trifluoroethanol for which no probe radius is available. Since propene epoxidation gave the same trends, only the corresponding naked reaction (**p,n**) served as a reference.

## Results

**Epoxidation of Ethene–RB3LYP Results. Clusters.** Preliminary GIAO-RB3LYP/6-311++G\*\* calculations, summarized in Supporting Information, confirm the NMR findings<sup>6a</sup> that the fluoro alcohol (R<sub>f</sub>OH) interacts with hydrogen peroxide by acting as both a proton donor and a proton acceptor. Two types of hydrogen-bonded clusters, H<sub>2</sub>O<sub>2</sub>–R<sub>f</sub>OH, were identified, the most stable ones of which are shown in Figure 1. The strength of the F···HO hydrogen bond can be assessed from the fact that the hydrogen bonded cluster of H<sub>2</sub>O<sub>2</sub>–CH<sub>3</sub>OH (Figure 1) yields approximately the same stabilization energy as the clusters of fluorinated alcohols and H<sub>2</sub>O<sub>2</sub> (7.1–7.9 kcal mol<sup>-1</sup>, see Figure 6). One may therefore deduce that F···HO bonds, as such, are rather weak, and any catalytic effect of the R<sub>f</sub>OH must originate from a special stabilization of the transition states.

**Transition States.** The RB3LYP transition states are shown in Figure 1. In the transition states, **TS(e,F3)** and **TS(e,F6)**, the R<sub>f</sub>OH chelates the departing OH moiety by a pair of hydrogen bonds. The hydroxyl group of R<sub>f</sub>OH acts as proton donor and the fluorine as an acceptor. The coordination around the oxygen of the departing OH becomes tetrahedral, while the hydrogen atom is directed toward the accepting fluorine, thus defining a ring structure with limited degrees of freedom, by reference to the transition structure for the reactions of the naked hydrogen peroxide, **TS(e,n)**, or the one coordinated to methanol, **TS(e,M)**. Two different conformations were located for the transition state for the **e,F3** combination. These two transition states are seen, from Figure 1, to differ in the number of F···H contacts, such that **TS(e,F3)'** is more compact and has more contacts than **TS(e,F3)**. We note that, although the F···H contacts are long, they are nevertheless important because of favorable electrostatic interactions that will be discussed later.

IRC calculations, starting from the transition structures **TS(e,n)** and **TS(e,F3)**, show that the reaction mechanism is invariably concerted, and as the O–O bond is broken, the departing OH group captures the hydrogen atom of the hydroxyl group of the HO···C=C moiety, thereby resulting in the products, epoxide and water molecule. The IRC starting from **TS(e,F3)** is shown in Figure 2. The same information is evident from the imaginary modes of the TSs in Figure 3. Thus, these transition states describe *nonsynchronous-concerted epoxidation mechanisms*.

**Epoxidation of Propene–RB3LYP Results.** Since propene epoxidation can have in principle Markovnikoff and anti Markovnikoff TSs, we performed an initial screening of the TSs for the epoxidation by naked hydrogen peroxide, reaction (**p,n**), using the RB3LYP/6-311G\* level. The four TSs are depicted in Figure 4, two Markovnikoff and two anti-Markovnikoff types, where the pair in each type differ in the relative orientation of the CH<sub>3</sub> and attacking-OH moieties, labeled as *cis* and

(21) Gordon, M. S.; Jensen, J. H. *Acc. Chem. Res.* **1996**, *29*, 536–543.

(22) Gonzales, C.; Schlegel, H. B. *J. Chem. Phys.* **1989**, *90*, 2154–2161.

(23) Reed, A. E.; Curtiss, L. A.; Weinhold, F. *Chem. Rev.* **1988**, *88*, 899–926.

(24) *Jaguar* 4.1, Schrödinger Inc.: Portland, OR, 2001.

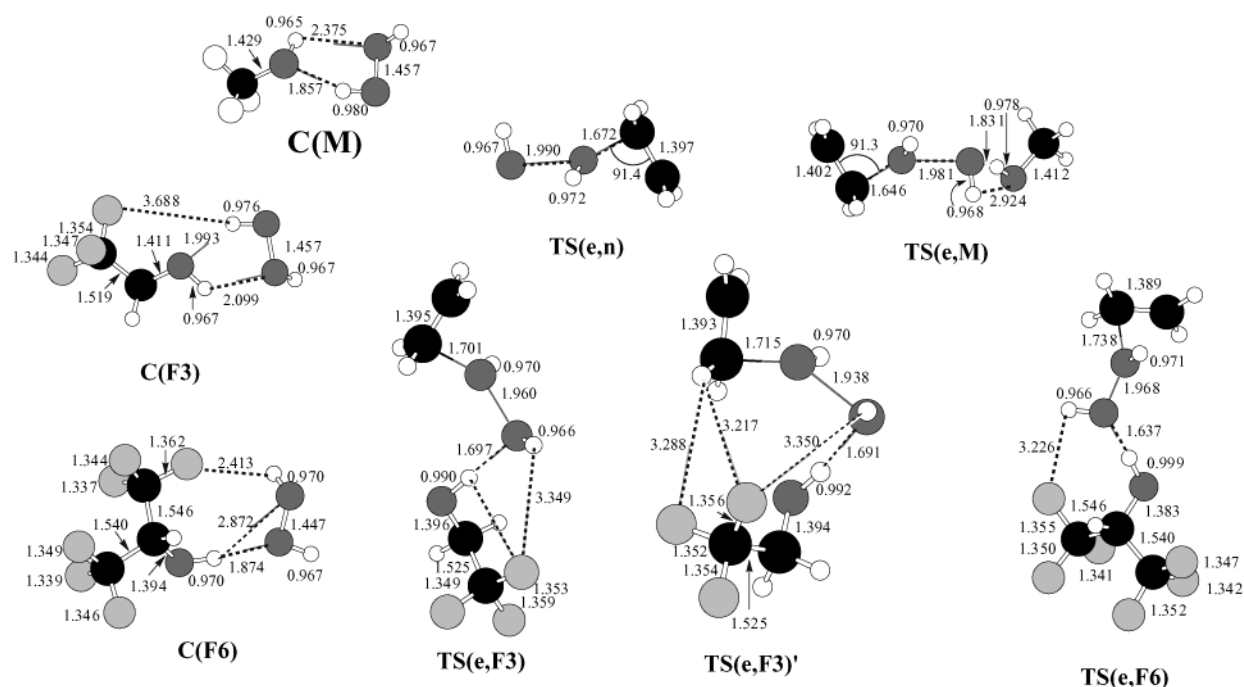


**FIGURE 1.** RB3LYP/6-311++G\*\* calculated clusters of fluorinated alcohols and  $\text{H}_2\text{O}_2$ , and transition structures for ethene epoxidation by “naked”  $\text{H}_2\text{O}_2$  and in the presence of methanol and fluorinated alcohols, labeled as described in the text. Distances are given in Å, and angles are in degrees.

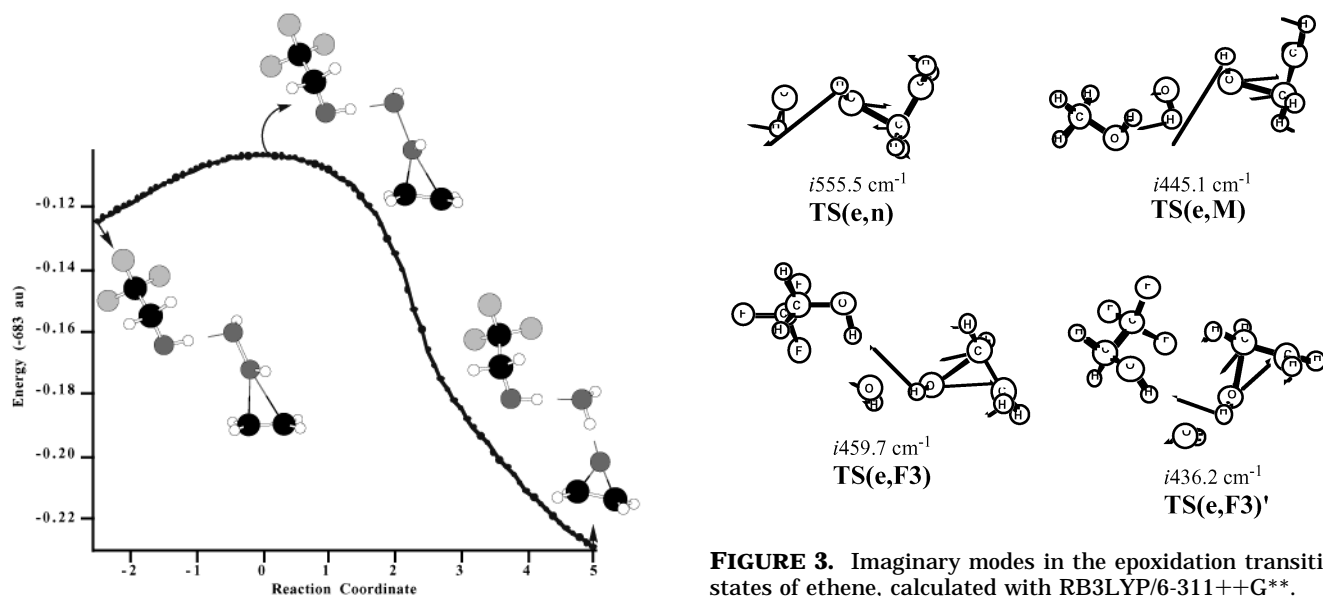


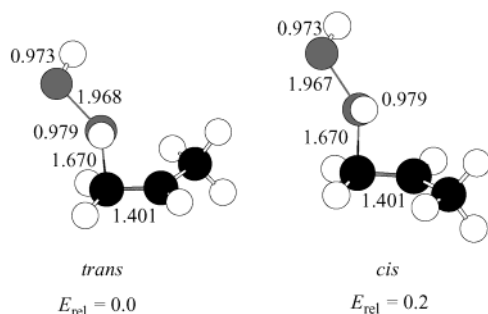
**FIGURE 2.** IRC profile for ethene epoxidation by  $\text{H}_2\text{O}_2$  in  $\text{CF}_3\text{-CH}_2\text{OH}$ , calculated with RB3LYP/6-311++G\*\*.

*trans*. Because all these TSs of the reaction (**p,n**) lie within a  $1.3 \text{ kcal mol}^{-1}$  range of energy, only the most stable one (the *trans*-Markovnikoff) was reoptimized at the RB3LYP/6-311++G\*\* level and is shown in Figure 5.

Figure 5 shows the most stable TSs for the different reactions of naked  $\text{H}_2\text{O}_2$  and  $\text{H}_2\text{O}_2\text{-R}_f\text{OH}$  coordinated reagent with propene. The corresponding  $\text{H}_2\text{O}_2\text{-R}_f\text{OH}$  clusters of fluorinated alcohols and  $\text{H}_2\text{O}_2$  are the same as the ones presented in Figure 1. As before, here too the fluoro alcohol conformation about the TS is variable,

and for the reaction (**p,F3**) we located two conformations, labeled as **TS(p,F3)** and **TS(p,F3)'**. The former is  $0.5 \text{ kcal mol}^{-1}$  more stable than the latter as a result of additional interactions between the substrate and the fluoro alcohol. As in the case of ethene, the  $\text{R}_f\text{OH}$  chelates the departing OH moiety by a pair of hydrogen bonds and forms a ring structure with limited degrees of freedom in the corresponding propene transition states, **TS(p,F3)**, and **TS(p,F6)**, compared to the naked **TS(p,n)**. While IRC following for these larger systems was not carried out, the finding of single transition state species for each process and the similarities of the transition state structures to those in the reaction with ethene suggest

Markovnikoff:



anti-Markovnikoff:

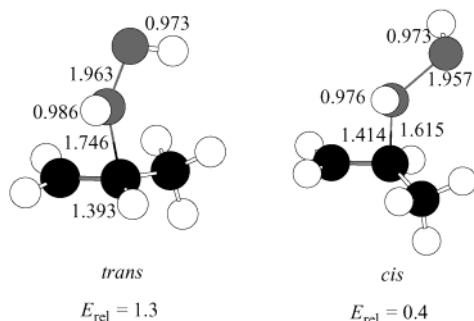


**FIGURE 4.** Markovnikoff and anti-Markovnikoff concerted nonsynchronous transition states for the reaction (p,n) calculated at the RB3LYP/6-31G\* level. The labels *cis* and *trans* correspond to the CH<sub>3</sub> and the attacking OH groups.

that much as for ethene the mechanisms for propene correspond to *nonsynchronous concerted epoxidations*.

**Energy Profiles for Concerted Epoxidation Reactions of Ethene and Propene.** Schematic reaction energy profiles for ethene and propene epoxidations at the RB3LYP/6-311++G\*\* level are summarized in Figure 6. The energies are reported relative to the reactants, where the energy is defined as zero. The RB3LYP mechanism describes a concerted epoxidation reaction, whereby in a single step the  $\pi$ -bond is activated and simultaneously the departing HO group of the hydrogen peroxide abstracts a proton from the attacking OH and leads to ring closure of the epoxide.

Table 1 summarizes the classical barriers and free energies of activation for epoxidation of the two alkenes, and more details are given in Supporting Information. It is apparent that the trends at the energy and free energy scales are identical.

**Epoxidation of Ethene and Propene—UB3LYP Results.** Stability tests of the RB3LYP TSs showed all of them to be unstable relative to the lower energy UB3LYP solutions (energy data are discussed later). Even though the energy differences are rather small (see later), one may wonder what is the mechanistic situation predicted by the UB3LYP method. To answer, we re-optimized two transition state species, **TS(e,n)** and **TS(e,F3)**, with the UB3LYP method and characterized their structures, which are displayed in Figure 7. Comparison to the corresponding RB3LYP structures in Figure 1 show great similarity, with the exception of the bond activation parameters ( $R_{\text{C}=\text{C}}$ ,  $R_{\text{O}=\text{O}}$ ,  $R_{\text{O}=\text{C}}$ , and  $\angle\text{OCC}$ ), which exhibit slightly “earlier” UB3LYP-TSs.

IRC following from the UB3LYP species correlated to the intermediates, **DR(e,n)** and **DR(e,F3)**. On the basis of the spin density distribution, these intermediates consist of a  $\beta$ -hydroxy ethyl radical and an OH radical; the latter species is either naked or coordinated to the fluoro alcohol. Thus, UB3LYP predicts that the first step of the reaction involves bond homolyses in both the olefin and the hydrogen peroxide. In a subsequent step, the intermediate undergoes hydrogen atom transfer to the departing OH group and undergoes ring closure to epoxide. In the case of the naked reaction we could not locate a transition state, and in all attempts the **DR(e,n)** intermediate collapsed to the epoxide plus water in a barrierless fashion. In the reaction with trifluoroethanol, we were able to locate a ring closure transition state, **TS<sub>rc</sub>(e,F3)**, with a ring closure barrier of 0.3 kcal/mol.

The entire reaction profiles at the UB3LYP level are depicted in Figure 8. They exhibit *seemingly stepwise* mechanisms, where the  $\beta$ -hydroxy ethyl/OH $\cdot$  radical pair encounters a barrier to ring closure. In the bare system we were not able to locate the ring closure transition state. However, the barrier is vanishingly small, as would be expected for hydrogen abstraction by hydroxyl radical, a reaction that approaches diffusion control.<sup>25</sup> It follows therefore that the UB3LYP mechanism predicts a diradical mechanism that is effectively concerted. However, because there is a diradical, albeit in a very shallow minimum, it may also escape the cage and give rise to small amounts of side reactions, such as allylic oxidation, especially when using sensitive substrates such as cyclohexene that are known to undergo allylic hydroxylation in diradical oxidation mechanisms. Such allylic oxidation was, however, not observed experimentally.<sup>6</sup> It is interesting that in the diradical mechanism as well the fluoro alcohol is found to lower the barrier considerably, so that the conclusions regarding the effect of the fluoro alcohol are very similar for RB3LYP and UB3LYP; *the fluoro alcohol lowers the barrier for oxidation in whatever mechanism*.

**Polar or Diradical: What is the Correct Mechanism?** To resolve this mechanistic dilemma, we decided to inspect the UB3LYP-RB3LYP relative energies under different conditions. Table 2 collects the relative UB3LYP-RB3LYP energies of the TS species and shows the spin contamination ( $\langle S^2 \rangle$ ) and group spin densities ( $\rho$ ) for the UB3LYP species. From the spin density data, it is apparent that for the naked species, **TS(e,n)** and **TS(p,n)**, as well as for the methanol coordinated one, **TS(e,M)**, the electronic structure resembles a singlet diradical with opposite spins on the departing OH group and the terminal carbon of the attacked double bond. However, in the species with fluorinated alcohol the diradical character gets smaller, especially so for the reactions of propene, where in **TS(p,F3)** and **TS(p,F6)** the diradical character is quite small. Furthermore, the energy difference,  $\Delta E_{\text{RB3LYP-UB3LYP}}$ , between the open and closed-shell solutions show clearly that, whereas in the naked transition states and the one coordinated by methanol the UB3LYP solution is significantly lower in energy than the RB3LYP by ca. 5 kcal mol<sup>-1</sup>, in the species coordi-

(25) The rate constant is approximately 10<sup>10</sup> M<sup>-1</sup> s<sup>-1</sup>. See, for example, Figures 1.7 and 1.8. Mayer, J. M. in *Biomimetic Oxidations Catalyzed by Transition Metal Complexes*; Meunier, B., Ed.; Imperial College Press: London, 2000; pp 1–44.

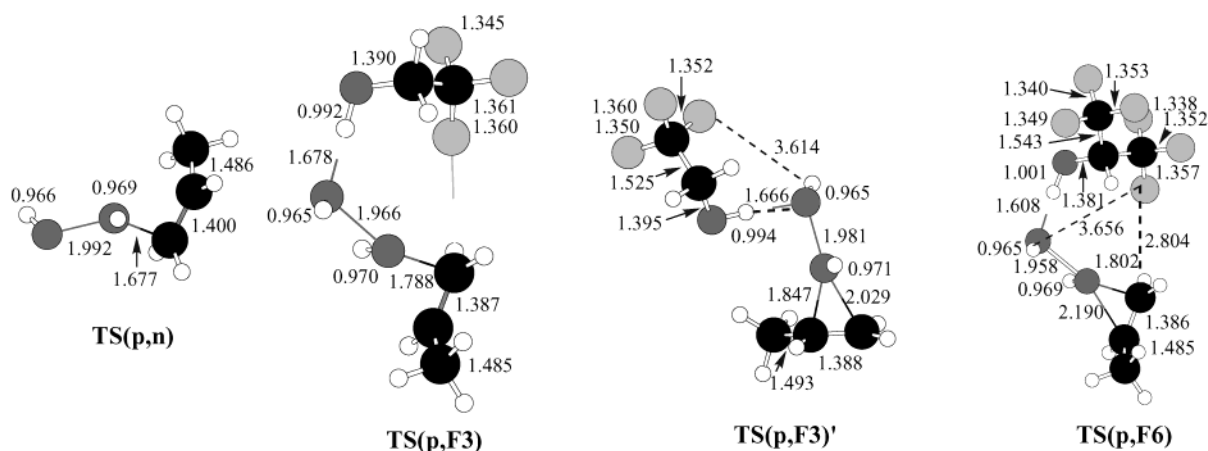


**FIGURE 5.** RB3LYP/6-311++G\*\* transition state structures for propene epoxidation by “naked” H<sub>2</sub>O<sub>2</sub> and in the presence of fluorinated alcohols. Distances are in Å, and angles are in degrees.

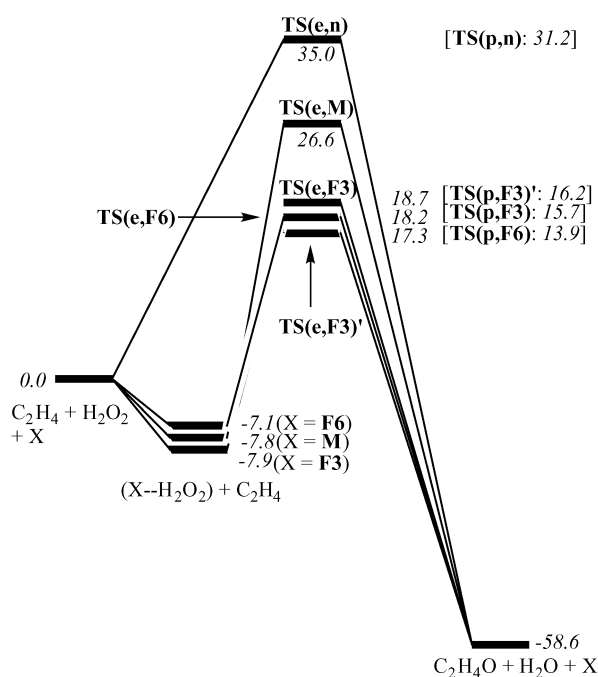


**FIGURE 6.** RB3LYP/6-311++G\*\* energy profiles for ethene epoxidation by “naked” H<sub>2</sub>O<sub>2</sub> and in the presence of methanol and fluorinated alcohols. The energies of the corresponding TSs of propene epoxidation measured from the corresponding reactants are shown on the right-hand side.

**TABLE 1.** RB3LYP/6-311++G\*\* Classical and Free Energy Barriers of Ethene and Propene Epoxidation by H<sub>2</sub>O<sub>2</sub> in the Gas Phase and in Fluorinated Alcohols

reaction	ethene (e)		propene (p)	
	$\Delta E^\ddagger$ <sup>a</sup> (kcal mol <sup>-1</sup> )	$\Delta G^\ddagger$ (kcal mol <sup>-1</sup> )	$\Delta E^\ddagger$ <sup>a</sup> (kcal mol <sup>-1</sup> )	$\Delta G^\ddagger$ (kcal mol <sup>-1</sup> )
<b>n</b>	35.0	43.7	31.2	40.4
<b>F3, F3'</b>	18.7, 17.3	38.4; 38.6	15.7, 16.2	37.7; 37.8
<b>F6</b>	18.2	38.9	13.9	33.3
<b>M</b>	26.6	44.2		

<sup>a</sup>  $\Delta E^\ddagger = \Delta E^\ddagger(\text{reactants} \rightarrow \text{TS})$ ;  $\Delta G^\ddagger = \Delta G^\ddagger(\text{reactants} \rightarrow \text{TS})$ .

nated with fluoro alcohols the difference is either small, ca. 1–2 kcal mol<sup>-1</sup>, or entirely insignificant, 0.05–0.39 kcal mol<sup>-1</sup>. These differences are too close to favor the

UB3LYP picture, especially since the data shows that the RB3LYP mechanism is affected by the relative polarity of the reactants and by the presence of the fluoro alcohol. Apparently, the fluoro alcohol endows the TSs with a polar character that increases with the donor ability of the olefin.

The data in Table 3 show the effect of solvent polarity on the  $\Delta E_{\text{RB3LYP-UB3LYP}}$  quantity as a function of two different dielectric constants; the value  $\epsilon = 1$  corresponds to the in-vacuum calculations (i.e., the gas-phase process). It is seen that in all cases the RB3LYP solution approaches closely the UB3LYP one to within 2 kcal mol<sup>-1</sup>. Moreover, for the reactions containing the fluoro alcohol there is an inversion of the relative ordering; the RB3LYP species attains the lower energy. Clearly, *the reactions assisted by the fluoro alcohols prefer the polar concerted mechanism predicted by the RB3LYP results.*

With these small energy differences and the inversion of the UB3LYP–RB3LYP ordering in the case of the fluoro alcohol containing TSs, one must not put the burden of mechanistic decision entirely on technical procedures such as the “stable” option in GAUSSIAN. Some chemical judgment is necessary to assess the two mechanisms. It is very clear that the RB3LYP and UB3LYP results are not mere artifacts but represent two chemically viable mechanisms that are different in terms of electronic structure. As revealed from a valence bond analysis of such processes, the electrons “flow” differently in the two mechanisms.<sup>26</sup> One mechanism, emerging from UB3LYP, predicts a mechanism with bond homolysis steps. By contrast, the second mechanism, emerging from RB3LYP, predicts a mechanism that exhibits characteristics of a polar reaction. In the polar mechanism, the departing HO will eventually acquire a hydroxide-like character by accepting an electron from the attacked  $\pi$ -bond<sup>26</sup> and will thereby deprotonate the hydroxyethyl and hydroxypropyl moieties en route to ring closure. Thus, these are two chemically distinct mechanisms, which because of their energy proximity are also legitimate *mechanistic alternatives that may coexist under real conditions.* In the naked and methanol coordinated processes, the diradical mechanism may prevail, and by

(26) Shaik, S.; Shurki, A. *Angew. Chem., Int. Ed.* **1999**, *38*, 586–625.

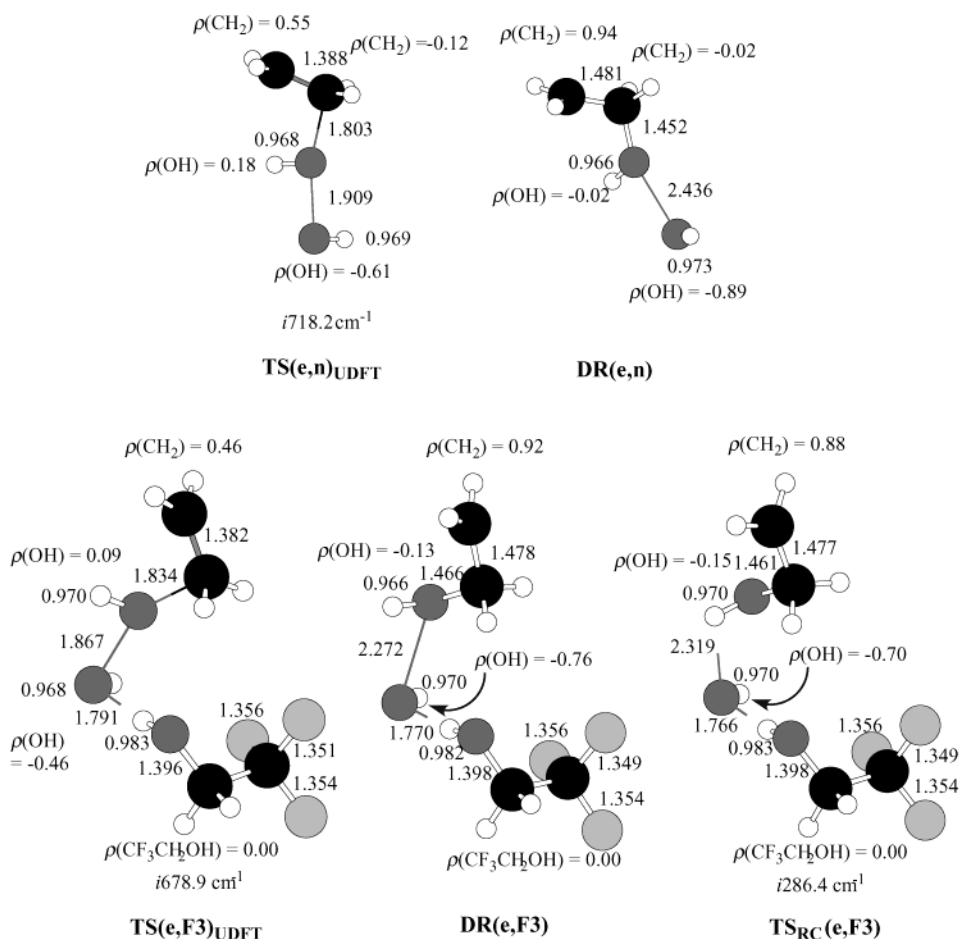


**FIGURE 7.** UB3LYP/6-311++G\*\* optimized geometries for the stepwise mechanisms of ethene epoxidation by H<sub>2</sub>O<sub>2</sub> (top) and in the presence of CF<sub>3</sub>CH<sub>2</sub>OH (bottom).

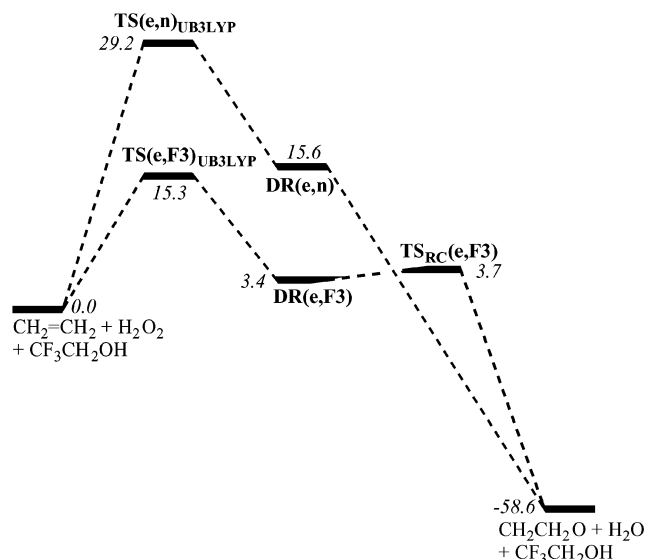


**FIGURE 8.** Potential energy profile for the diradical mechanism (UB3LYP) of ethene epoxidation by H<sub>2</sub>O<sub>2</sub> and in the presence of CF<sub>3</sub>CH<sub>2</sub>OH (bottom). Note that these are effectively concerted mechanisms.

contrast, in the fluoro alcohol assisted reactions the concerted polar mechanisms are likely to prevail. The experimental data does not detect any reactivity in

nonfluorinated alcohols,<sup>6</sup> whereas in the presence of the fluoro alcohols the reactions are stereospecific and exhibit other characteristics of a polar mechanism. Clearly therefore, the available experimental data for the stepwise diradical mechanism and favor a concerted polar mechanism. Guided by the experimental results, we consider henceforth the polar mechanism and attempt to understand the catalytic effect of the fluoro alcohols.

## Discussion

The RB3LYP calculations show that epoxidation of ethene and propene by H<sub>2</sub>O<sub>2</sub>, free or coordinated to an alcohol molecule, can proceed in a nonsynchronous but concerted manner. An additional characterization of the mechanism can be made by inspection of the charge distribution in the transition state. Figures 9 and 10 show the natural charges,<sup>23</sup> for all of the transition states. Thus, the amounts of charge transfer from the alkene to the hydrogen peroxide range from 0.24e to 0.39e for ethene and from 0.37e to 0.44e for propene, and in both cases the charge transfer increases markedly in the presence of the fluoro alcohol. Furthermore, the departing OH group is negatively charged, and its charge accounts for most of the charge transfer from the olefin. These features agree with earlier MP2, B3LYP, and CCSD results of Bach and co-workers<sup>2,5,27</sup> on olefin epoxidation

**TABLE 2. Results of Stability Calculations; B3LYP/6-311++G\*\***

TS	$\Delta E_{\text{RDFT-UDFT}}$ (kcal mol <sup>-1</sup> )	$\rho(\text{OH})^a$	$\rho(\text{OH})^b$	$\rho(\text{CH})^c$	$\rho(\text{CH}_2)^d$	$\rho(\text{CH}_3)^e$	$\rho(\text{R})^f$	$\langle S^2 \rangle$
<b>TS(e,n)</b>	-5.27	0.05	-0.64	-0.09	0.71			0.582
<b>TS(e,M)</b>	-4.64	0.00	-0.59	-0.05	0.65		0.00	0.553
<b>TS(e,F3)</b>	-2.25	0.01	-0.50	-0.04	0.52		0.00	0.410
<b>TS(e,F3)'</b>	-2.26	0.01	-0.50	-0.05	0.53		0.00	0.416
<b>TS(e,F6)</b>	-1.13	0.02	-0.42	-0.02	0.42		-0.01	0.298
<b>TS(p,n)</b>	-5.40	-0.01	-0.63	-0.07	0.69	0.01		0.589
<b>TS(p,F3)</b>	-0.05	-0.03	0.21	-0.01	-0.16	0.00	0.00	0.066
<b>TS(p,F6)</b>	-0.39	0.03	-0.34	0.00	0.29	0.00	0.00	0.184

<sup>a</sup> OH donor group of H<sub>2</sub>O<sub>2</sub>. <sup>b</sup> OH rest group of H<sub>2</sub>O<sub>2</sub>. <sup>c</sup> CH group of ethene or propene that binds oxygen. <sup>d</sup> CH<sub>2</sub> group of ethene/propene. <sup>e</sup> CH<sub>3</sub> group of propene. <sup>f</sup> R represents methanol/trifluoro ethanol or hexafluoropropanol.

**TABLE 3. Energy Differences of RDFT and UDFT Calculated Transition States in the Gas Phase ( $\epsilon = 1$ ) and in Solvents ( $\epsilon = 5.7$ ;  $\epsilon = 10.65$ )<sup>a</sup>**

TS	$\Delta E_{\text{UDFT-RDFT}}$ (kcal mol <sup>-1</sup> )		
	$\epsilon = 1$	$\epsilon = 5.7$	$\epsilon = 10.65$
<b>TS(e,n)</b>	-5.26	-2.30	-1.56
<b>TS(e,M)</b>	-4.64 <sup>b</sup>	-4.61 <sup>b</sup>	+0.18
<b>TS(e,F3)</b>	-2.24	-0.72	-0.60
<b>TS(e,F3)'</b>	-2.29	-0.95	-0.84
<b>TS(e,F6)</b>	-1.12	-0.10	+0.21
<b>TS(p,n)</b>	-5.37	-2.88	-2.34
<b>TS(p,F3)</b>	-0.03	+0.02	+0.09
<b>TS(p,F6)</b>	-0.14	+0.11	+0.07

<sup>a</sup> All data taken from Jaguar 4.1. <sup>b</sup> The value is obtained by using the gas-phase energy gap from Gaussian 98. Jaguar 4.1 seems to overestimate the UDFT energy for this reaction. Since there is no STABLE option in JAGUAR, we could not test the stability of the UDFT solution itself within JAGUAR.

by peroxy-carboxylic acids. Clearly, in line with our foregoing analysis in the Results section, RB3LYP theory predicts a polar epoxidation mechanism. Another indication for the polar nature of the mechanism is provided by the data in Table 1, which reveal that the computed activation energies for propene epoxidation are lower than for ethene epoxidation, at either energy or the free energy scales. Therefore, *the DFT calculations reveal a polar mechanism that acquires enhanced ionicity in the presence of a fluoro alcohol and proceeds in a concerted, albeit nonsynchronous, manner.* This conclusion accords with experimental results, which demonstrate that the process catalyzed by fluoro alcohol is stereoselective<sup>6a</sup> and the more nucleophilic olefins exhibit higher epoxidation reactivity.<sup>6,7</sup>

Inspection of the energy barriers in Figure 6 and Table 1 reveals that fluorinated alcohols catalyze the epoxidation by ca. 16–18 kcal mol<sup>-1</sup> with respect to the reference gas-phase reactions, (e,n) and (p,n). Using the (e,M) reference, the effect is reduced but remains substantial at 8.0–9.3 kcal mol<sup>-1</sup>. At the free energy scale the catalytic effect is ca. 5–6 kcal mol<sup>-1</sup> for ethene epoxidation and 2.6–6.9 kcal mol<sup>-1</sup> for propene epoxidation. Furthermore, calculations confirm that, for the same number of F...H contacts in the TS (i.e., compare **TS(p,F3)** to **TS(p,F6)**), (CF<sub>3</sub>)<sub>2</sub>CHOH is a better catalyst than CF<sub>3</sub>CH<sub>2</sub>OH, in accordance with experiment.<sup>6,7</sup>

To ascertain that the catalytic effect is not simply an effect of solvent polarity, which is mimicked by the

presence of the alcohol, we performed single point calculations, of the clusters and TSs of the reference and catalyzed reactions, **TS(e,M)**, and **TS(e,F3)**, in a dielectric environment.<sup>24</sup> To obtain a reliable trend we used two different dielectric constants of 5.7 and 10.65, which bracket the dielectric constant of fluoroethanol, 8.55. The results, in Table 4, show that solvation reduces all of the barriers, in line with the polar nature of the mechanisms. Nevertheless, the trend remains as was noted for the unsolvated species; the fluoro alcohol is seen to catalyze the reaction by 5.2–7.9 kcal mol<sup>-1</sup>, which translates roughly to between 4 and 6 orders of magnitude at 300 K.

#### Origins of Catalytic Effect by Fluoro Alcohols.

Since F...HO hydrogen bonding interactions were found to be very small for the ground state clusters, the effect of fluoro alcohol on the transition state cannot be simply ascribed to hydrogen bonding with the fluoro substituents of the alcohol. Inspection of the geometries of the transition states and their charge distribution provides some insight into the catalytic effect. The geometries of the three TSs (Figures 1, 5, and 7) reveal that the uncatalyzed reactions undergo generally a higher degree of bond elongation in the bonds that are broken, C=C and O–O, and a more advanced O–C bond formation, compared with TSs coordinated by fluoro alcohols, which are earlier TSs. In addition, the hydrogen atom that has to migrate to the departing hydroxyl group to form water and epoxide is more favorably oriented for this migration in the presence of the fluoro alcohol in the TS (see Figures 1 and 4). Thus, the fluoro alcohol reduces the deformation energy of the reacting fragments in the TS and imposes structural organization on the TS, via the cyclic hydrogen bonded array.

Another important effect is the stabilization of the TSs by the various O...H and F...H contacts. Significant geometric changes are observed in the initial hydrogen bonds of the fluoro alcohol coordinated TSs vis-à-vis the corresponding clusters. For example, the R<sub>1</sub>OH...O distances are ca. 15% shorter in the **TS(e,F3)** and **TS(e,F6)** compared to their respective clusters, **C(F3)** and **C(F6)**. Furthermore, as shown in Figures 9 and 10, the presence of fluorinated alcohol noticeably amplifies the amplitudes of charge alternation in transition structures for ethene and propene epoxidations. In turn, the fluoro alcohol juxtaposes the positively charged hydroxylic hydrogen against the negatively charged oxygen of the departing OH group, while the positively charged hydrogen of the latter group feels the negatively charged fluorine. The charge on the fluorine substituents is

(27) Bach, R. D.; Glukhovtsev, M. N.; Gonzalez, C.; Marquez, M.; Estevez, C. M.; Baboul, A. G.; Schlegel, H. B. *J. Phys. Chem. A* **1997**, *101*, 6092.

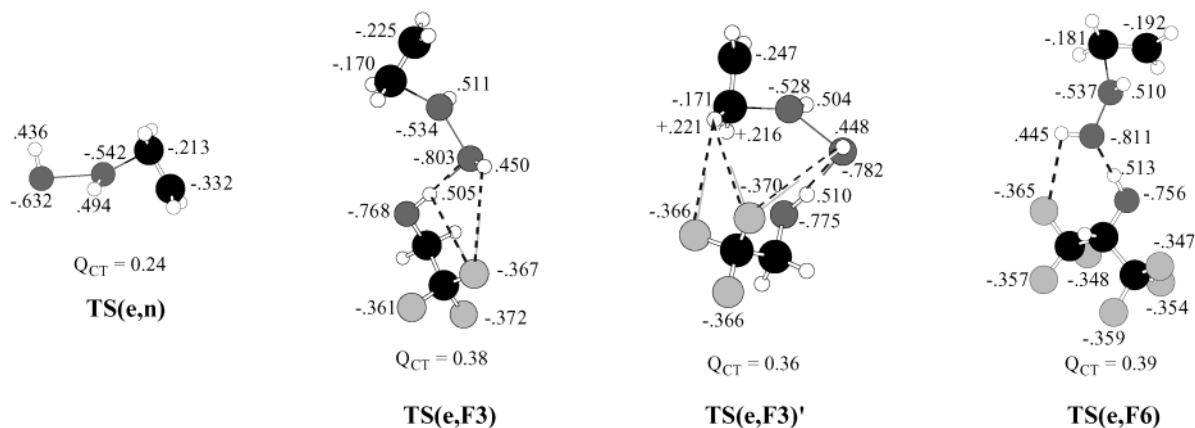


FIGURE 9. Natural charges for the TSs of ethene epoxidation.

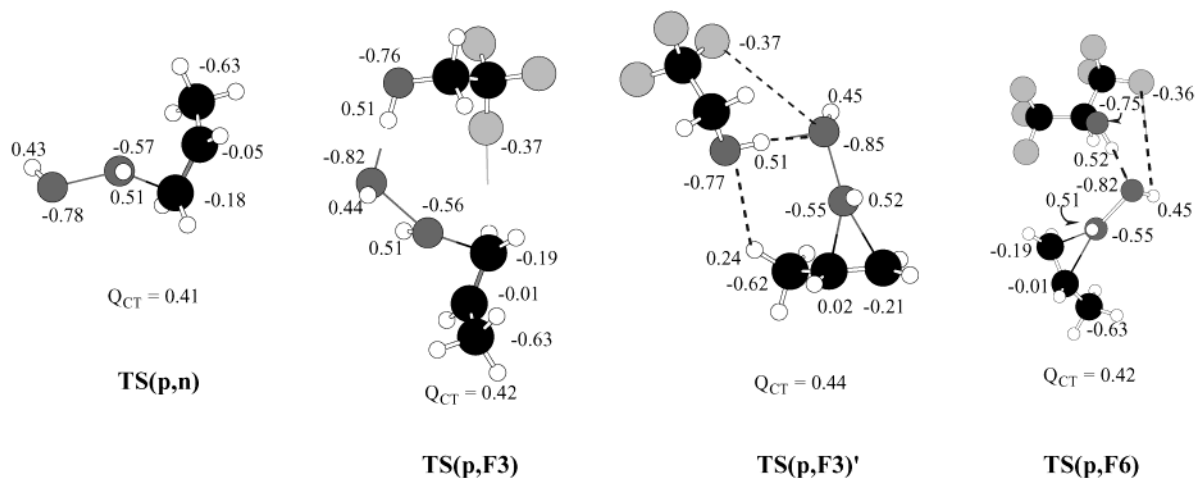


FIGURE 10. Natural charges for the TSs of propene epoxidation.

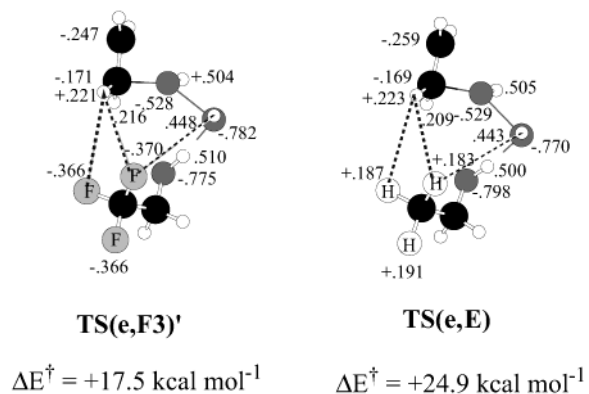
TABLE 4. Effect of Continuum Solvation on Free Barriers of Ethene Epoxidation

reaction	$\Delta G^\ddagger$ (cluster $\rightarrow$ TS), 300 K		
	$\epsilon = 1^{a,b}$	$\epsilon = 5.7^{a,c}$	$\epsilon = 10.65^{a,c}$
<b>F3</b>	33.4	26.6	25.8
<b>F3'</b>	33.7	29.2	28.8
<b>M</b>	42.1	34.4	33.0

<sup>a</sup>  $\epsilon$  is a dielectric constant,  $\epsilon = 1$  corresponds to the gas-phase conditions. <sup>b</sup> The gas-phase free energy is calculated with Gaussian 98. <sup>c</sup> Solvation energies calculated with Jaguar 4.1. The  $T\Delta S^\ddagger$  term is added from the gas-phase calculations.

significant ( $-0.36$  to  $0.38e$ ), and their juxtaposition against substantially positive charges, e.g.,  $+0.45e$  on the hydrogens, causes significant *electrostatic stabilization*, even if the  $F\cdots H$  distances are rather long. An interesting comparison that illustrates this effect is the relative energy of **TS(e,F3)** and **TS(e,F3)'** in Figure 6. Thus, in the more compact **TS(e,F3)'** the fluoro substituent has additional interactions with the positively charged hydrogens (charge =  $+0.22e$ ) of the ethene moiety. These interactions are missing in **TS(e,F3)**, and hence its energy is  $1.2 \text{ kcal mol}^{-1}$  higher than that of **TS(e,F3)'**. Thus, the fluoro alcohol enhances the charges of the transition states and *causes electrostatic catalysis by acting as a charge template of the transition states*.

SCHEME 2. Natural Charges in **TS(e,F3)'** and Its Analog **TS(e,E)** Generated by Replacing the Trifluoroethanol by Ethanol<sup>a</sup>



<sup>a</sup> Also shown are the  $\Delta E^\ddagger$  energies of these TSs relative to the separated reactants (see Figure 6).

The special role of the negative charge on the fluoro substituent can be contrasted with a nonfluorinated alcohol. Scheme 2 shows charge distributions in **TS(e,F3)'** and **TS(e,E)** that were generated by replacing the trifluoroethanol by ethanol, while keeping all other geometric parameters fixed. It is seen that *whereas*

trifluoroethanol is a compatible charge template of the epoxidation TS, ethanol is incompatible because the methyl hydrogens of ethanol are all positively charged and undergo repulsive interactions with the epoxidation TS, thereby raising the barrier by ca. 7 kcal mol<sup>-1</sup>. With this charge complementarity the fluoro alcohol functions such as a tiny enzyme. The notion of charge complementarity is lucid enough to design other templating solvents, e.g., based on silicon derivatives.

To summarize, the fluoro alcohol catalyzes the epoxidation reaction by inducing a combination of effects. First, it reduces the geometric deformations of the olefin and the hydrogen peroxide in the TS. Second, it intensifies the R<sub>f</sub>OH...H hydrogen bonding donated by the alcohol. Third, it increases the charge alternation of the TS and acts as a complementary charge template that provides electrostatic stabilization to the hydrogen peroxide and olefin moieties of the TS. This combination reduces the reaction barrier by a factor sufficiently large to render the concerted epoxidation observable under mild synthetic conditions. Thus, as a result of the polar nature of the mechanism, *the fluoro alcohol provides a charge template, complementary to H<sub>2</sub>O<sub>2</sub>-alkene moiety, and thereby brings about a specific stabilization of the transition state of olefin epoxidation.*

## Conclusions

The DFT calculations provide two alternative mechanisms for alkene epoxidation by hydrogen peroxide; one occurs via bond homolysis of the peroxide and the  $\pi$ -bond and the other by a concerted polar mechanism. Fluoro alcohols such as hexafluoroisopropyl alcohol prefer the polar mechanism (Table 3). Inspection of the trends computed for the polar mechanism show that the recent observations<sup>6,7</sup> that alkene epoxidation by hydrogen peroxide can be achieved under mild conditions in fluorinated alcohols originate in a catalytic effect due to the participation of the fluoro alcohol in the transition state. The calculations reproduce experimental trends, such as the stereospecificity of the epoxidation, the enhanced rate of electron richer olefins, and the higher effectiveness of (CF<sub>3</sub>)<sub>2</sub>CHOH compared with trifluoroethanol.<sup>6</sup> Analyses of the transition states show that catalysis by fluoro alcohol is due to three main factors. Geometrically, the presence of the fluoro alcohol reduces the bond deformations of the alkene and hydrogen peroxide in the transition state. Electronically, the fluoro

alcohol increases the polarity of the transition state and acts as a complementary charge template to the hydrogen peroxide and olefin moieties in the transition state. This charge complementarity of the fluoro alcohol stabilizes the transition state by electrostatic interactions, especially between the negatively charged fluoro substituents and the positively charged hydrogens of the alkene and the hydrogen peroxide. This template catalysis is reminiscent of the “push–pull” activation of hydrogen peroxide in peroxidase heme-enzymes.<sup>28</sup> Recent results by Schreiner and Wittkopp<sup>29</sup> demonstrated that urea can replace Lewis acids to catalyze Diels–Alder reactions and 1,3-dipolar cycloadditions, by acting as a hydrogen bonding template to the corresponding transition state. Clearly, the effect found in this study is just part of the growing recognition that charge templates, which employ hydrogen bonds, have favorable effects on chemical reactivity.<sup>30–33</sup>

The diradical mechanism exhibits also a clear catalytic effect of the fluoro alcohol (Figure 8). However, as yet there is no experimental evidence that supports a diradical bond homolysis mechanism of alkene epoxidation by hydrogen peroxide. Nevertheless, because this mechanism is predicted to be close in energy to the concerted polar mechanism, it must be considered and be either verified or falsified by experimental means.

**Acknowledgment.** The research is supported by the Ministry of Science, Culture and Sports of Israel. R.N. is the Israel and Rebecca Sieff Professor of Organic Chemistry.

**Supporting Information Available:** Tables with calculated gas-phase and solvent reaction energies at different computational levels; tables of H<sub>2</sub>O<sub>2</sub>–R<sub>f</sub>OH cluster energies and their NMR properties; figures with structures and charges at various levels. This material is available free of charge via the Internet at <http://pubs.acs.org>.

JO034087T

(28) Sono, M.; Roach, M. P.; Coulter, E. D.; Dawson, J. H. *Chem. Rev.* **1996**, *96*, 2841–2888.

(29) (a) Schreiner, P. R.; Wittkopp, A. *Org. Lett.* **2002**, *4*, 217–220.  
(b) Wittkopp, A.; Schreiner, P. R. *Chem. Eur. J.* **2003**, *9*, 407–414.

(30) Rouhi, M. *Chem. Eng. News*, **2002**, April 22, 3033.

(31) Tantillo, D.; Houk, K. N. *J. Comput. Chem.* **2002**, *23*, 84–95.

(32) de Visser, S. P.; Ogliaro, F.; Sharma, P. K.; Shaik, S. *Angew. Chem., Int. Ed.* **2002**, *41*, 1947–1951.

(33) de Visser, S. P.; Ogliaro, F.; Sharma, P. K.; Shaik, S. *J. Am. Chem. Soc.* **2002**, *124*, 11809–11826.